The Saudi Dental Journal 36 (2024) 340–346

Contents lists available at ScienceDirect

The Saudi Dental Journal

journal homepage: www.ksu.edu.sa
www.sciencedirect.com

Original Article

Cutting guides in mandibular tumor ablation: Are we as accurate as we think?

Omar Suhaym [a,*], Loren Moles [b], Nicholas Callahan [b]

[a] Maxillofacial Surgery and Diagnostic Sciences, King Saud Bin Abdulaziz University for Health Sciences, King Abdullah International Medical Research Center (KAIMRC), Prince Mutib Ibn Abdullah Ibn Abdulaziz Rd, Ar Rimayah, 14611 Riyadh, Saudi Arabia
[b] Oral and Maxillofacial Surgery, UIC, USA

ARTICLE INFO

Keywords:
Computer-assisted Surgery
VirtualSurgical Planning
Cutting guides

ABSTRACT

Purpose: Tumor margin status is critical in local tumor recurrence and is a significant prognostic factor in head and neck cancer survival. With the introduction of computer-assisted surgical planning, one of the main challenges is the accurate positioning of the surgical cutting guide but there is limited evidence of the accuracy of the 3D cutting guides in mimicking virtually planned osteotomy. This study evaluates the accuracy of osteotomy lines produced by 3D-printed cutting guides and assesses the overall accuracy of mandibular reconstruction.
Material and Methods: The pre and postoperative 3D models were aligned using an automated surface registration feature based on the iterative closest point algorithm. The differences in osteotomy line deviation, linear and angle measurements, and 3D volume quantification of the pre and post models were measured.
Results: We included 14 patients (8 men and 6 women with ages ranging from 13 to 75 years) with a segmental mandibular resection who met all of the inclusion criteria. The smallest defect size was 4.4 cm, the largest defect was 12.2 cm, and the average was 7.30 cm +/- 2.80 cm. The average deviation between virtually planned osteotomy and actual surgical osteotomy was 1.52 +/-1.02 mm. No covariates were associated with increased inaccuracy of the 3D-printed cutting guides.
Conclusion: The finding of this study suggests that virtual surgical planning is an unambiguous paradigm shift in the predictability of the surgical plan and achievement of the reconstruction goals. The 3D-printed cutting guides are a very accurate and reliable tool in translating virtual ablation plans to an actual surgical resection margin.

1. Introduction

The mandible is a unique structure with numerous crucial functions that affect quality of life. The complexity of oromandibular defects secondary to trauma or tumor ablation requires comprehensive assessments and treatment objectives to restore the facial form and function (Abou-ElFetouh et al., 2011; Ayoub et al., 2014).

The introduction of computer-assisted surgical planning and computer-aided manufacturing in reconstructive surgery has many advantages such as decreased operative and ischemic times and superior accuracy. (Bak et al., 2010; Bao et al., 2017; Barker et al., 1994) However, one of the main challenges is the accurate positioning of the surgical cutting guide due to lack of anatomical landmarks and soft tissue interferences during placement. This remains even after the introduction of computer-assisted surgical planning.

To the best of our knowledge, no previous study has yet assessed the osteotomy line created by virtually planned 3D-printed guides. The importance of surgical margins cannot be overemphasized because of the tremendous consequences on cancer outcomes and the use of adjunctive therapy—this is especially true in oncological cases. (Barry et al., 2021; Brown et al., 2016) This is a retrospective cohort study to evaluate the accuracy of osteotomy lines produced by the virtually planned three-dimensionally printed cutting guides and to assess the overall accuracy of mandibular reconstruction using virtual planning and patient-specific reconstruction plates. We hypothesize that the virtually planned osteotomy lines do not match the actual surgical osteotomy.

* Corresponding author.
E-mail addresses: suhaymo@ksau-hs.edu.sa (O. Suhaym), smoles2@uic.edu (L. Moles), ncall@uic.edu (N. Callahan).

https://doi.org/10.1016/j.sdentj.2023.11.017
Received 21 July 2023; Received in revised form 13 November 2023; Accepted 15 November 2023
Available online 17 November 2023
1013-9052/© 2023 THE AUTHORS. Published by Elsevier B.V. on behalf of King Saud University. This is an open access article under the CC BY-NC-ND license (http://creativecommons.org/licenses/by-nc-nd/4.0/).

2. Materials and methods

2.1. Study population

This study was approved by the Institutional Review Board of the University of Illinois at Chicago (UIC IRB Protocol #2019–0836). We conducted a retrospective evaluation of all patients who had virtual surgical planning using IPS® KLS Martin and fabrication of 3D printed cutting guides for the ablation of mandibular pathology between July 2016 and June 2020. The inclusion criteria included patients who underwent a virtually planned mandibular resection, had complete preoperative and postoperative records, and had a high-resolution CT scan with a maximum slice thickness of 2 mm or CBCT; reconstruction included a custom-made cutting guide and patient-specific reconstruction plate obtained with CAD/CAM workflow. Any case that did not meet all the inclusion criteria were excluded.

2.2. Imaging acquisition and processing

The pre- and postoperative images were obtained using the same scanner and parameters. Eleven patients had cone-beam computer tomography (I-CAT, Imaging Sciences International, Hatfield, USA), while three patients had multiple detector computer tomography with a 0.5-mm pitch (256-slice CT scanner, GE Healthcare, Milwaukee, USA) in accordance with the bone acquisition protocol. The slice thickness was less than 1.25 mm to ensure there was no significant effect on volume measurements. (Chang et al., 2013; Choi et al., 2002) The first postoperative scan was acquired within six weeks from surgery and was selected for comparison to minimize the long-term changes in volume and position. (Ciocca et al., 2015) The scanned images were obtained in DICOM (Digital Imaging and Communications in Medicine) format for both the pre and postoperative scans and were processed using ProPlan CMF software.

2.3. 3D model orientation and superimposition

The preoperative 3D virtual models were acquired from the existing CAD/CAM protocol used for the virtual planning for each patient, while the DICOM file from the postoperative CBCT or CT scan were processed via ProPlan CMF ® software for segmentation, clean up, and to create postoperative 3D models comparable to the preoperative models. Next, the pre and postoperative 3D models were transferred to a 3D Slicer for alignment using the automated surface registration feature based on the iterative closest point algorithm. If the registration process was unsatisfactory, then landmark-based registration was performed to ensure adequate alignment between both models. The transferred model was saved in the new position and exported as an STL file for analysis.

The models were then transferred to Meshmixer to measure the deviation in the osteotomy lines. The XYZ orientation was based on the Frankfort plane, the midsagittal plane (perpendicular to Frankfort and crossing the nasion-basion), and the nasion. The models were then imported to MeshLab for volumetric analysis. The preoperative model was selected as a targeted mesh, and the distance was measured between the two meshes. The relationship between the two meshes was then preserved and colorized by vertex quality to visualize and quantify the volume deviation changes. Finally, a quality histogram was rendered to obtain the maximum, minimum, average, and percentage of the volume deviation.

2.4. Osteotomy line deviation

To measure the accuracy of the cutting guides, the manual superimposition of remnant mandible segments was labeled as small and large segments. Different planes were used to visualize the distance between the planned and the actual osteotomy lines; the largest distance was then measured perpendicular to the osteotomy line. Fig. 1 represents an example of the superimposition process.

2.5. Calculation of the linear measurements

Each model was analyzed individually during landmark identification, and the paired model was deselected to prevent any bias. Landmarks, length, and angle-identification protocol were adopted from De

Table 1
Landmarks, lengths, and angles used in the linear measurements.

Condylion	The most posterior superior point in the mandibular condyle.
Gonion	The most inferior point in the mandibular ramus.
Horizontal corner	The point at the intersection between the mandibular plane and mental foramen perpendicular.
Gnathion	Midpoint between pogonion and menton.
Intercondylar distance	The linear distance between condylion 1 and condylion 2.
Intergonial distance	The linear distance between gonion 1 and gonion 2.
Mandibular ramus length	The distance between condylion and gonion.
Mandibular body length 1	The distance between gonion and the horizontal corner.
Mandibular body length 2	The distance between gonion and gnathion.
Sagittal mandibular angle	The angle formed by the plane passing through the gonion and the horizontal corner and the plane passing through the gonion and condylion.

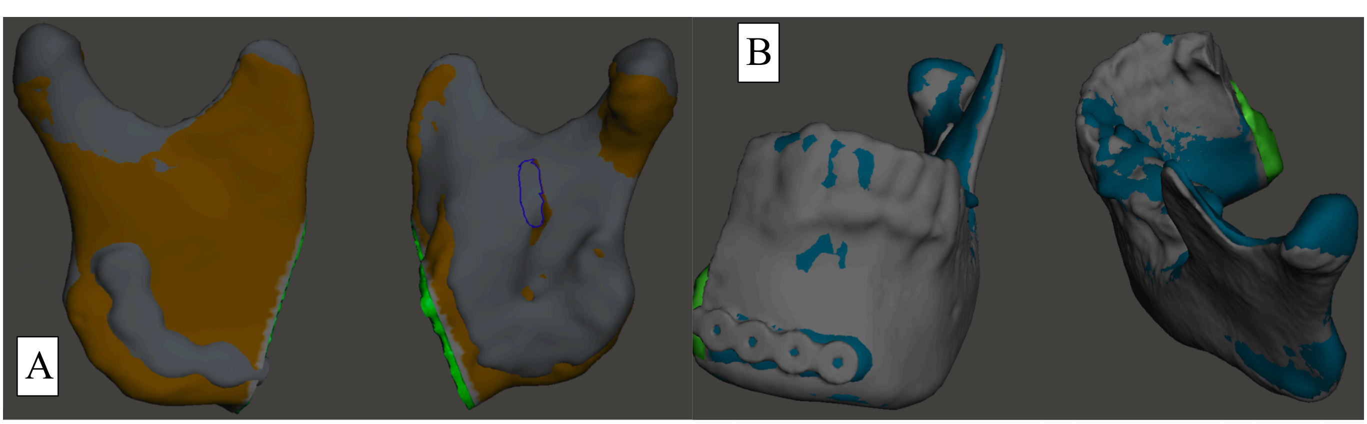

Fig. 1. Case example for osteotomy line deviation virtual versus surgical cut. A: small segment superimposition (Preoperative plan in brown, postoperative in gray), B: Large segment superimposition. (Preoperative plan in teal, postoperative in gray. Light green indicates the amount of discrepancy). (For interpretation of the references to color in this figure legend, the reader is referred to the web version of this article.)

Maesschalck et al. (Ciocca et al., 2016; De Maesschalck et al., 2017) with some modifications elucidated in Table 1. One side was randomly selected in the case of bilateral resection. The case was eliminated from the linear or angle analysis in the case of missing landmarks due to resection. Fig. 2 shows an example of the linear and angle measurements.

2.6. 3D volume quantification

A color map based on the vertex quality between the two models was generated automatically without cropping the outliers. The maximum positive value, maximum negative value, average deviation value, and percentage of the average value were recorded and compared to the preoperative mandibular model. Fig. 3 represents an example of the volumetric analysis.

2.7. Statistical analysis

IBM SPSS Statistics version 27.0 for macOS (IBM Corp., Armonk, NY, USA) was used for statistical data analysis. Descriptive statistics were computed for all demographic data, and the key variables with some variables were collapsed for better statistical representation such as diagnosis and location. All landmarks and measurements were repeated by the second author (LM). Interclass correlation coefficient (ICC) was adopted from Koo and Li (Disa et al., 1997) where an ICC value < 0.50 means poor reliability, 0.50–0.74 moderate reliability, 0.75–0.90 good reliability, and > 0.90 indicates excellent reliability. A one-sample *t*-test evaluated if the mean deviation was statistically different versus the reported average deviation in the literature (test deviation 2 mm); p-value < 0.05 was considered to be statistically significant. A paired-sample *t*-test examined if the mean deviation in the linear, angle, and volume were different between the virtual and the actual plan; p-value < 0.05 was considered significant.

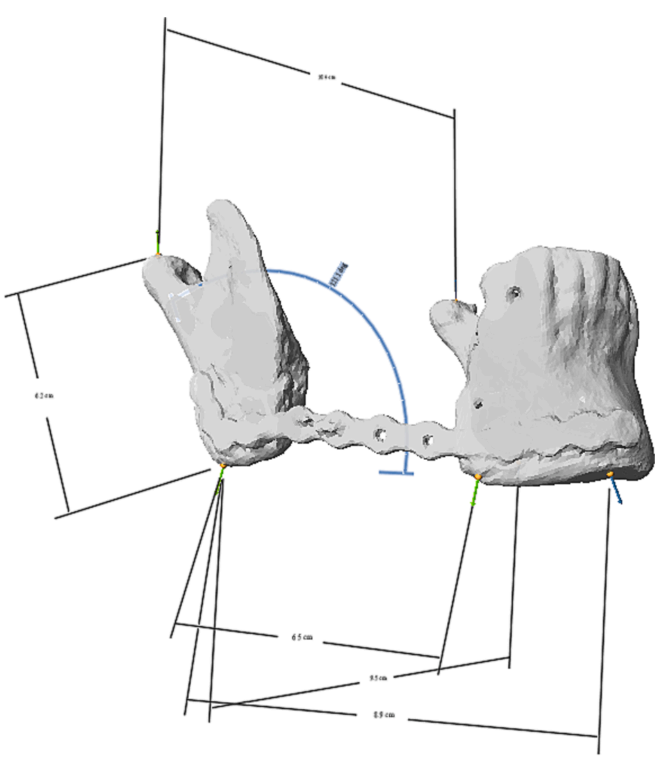

Fig. 2. Case example of landmark identification, linear distance, and sagittal angle measurement of the postoperative model.

3. Results

3.1. Patient demographics

The sample consisted of eight males and six females with ages ranging from 13 to 75 years with an average of 48.5 years. According to the Brown classification (Eljamel, 1997), three subjects had class I defects, two had class Ic, two had class II, four had class III, and three had class IV defects. The smallest defect size was 4.4 cm, the largest defect was 12.2 cm, and the average was 7.30 cm +/- 2.80 cm. The rest of the patient's demographics are listed in Table 2.

3.2. Osteotomy line deviation

The sample consisted of 26 mandibular osteotomies performed utilizing 3D-printed cutting guides. Of those, 12 were on the small segment and 14 were on the large residual segment. The average deviation between the virtually planned cut and the actual surgical osteotomy was 1.52 +/- 1.02 mm. The range of deviations in the small segments was between 0.1 and 3.8 mm with a mean of 1.3 +/- 1.04. In contrast, the discrepancy in the large segments was 0.2–3.7 mm with an average of 1.85 +/- 1.06 mm. The difference in the deviation in both small and large segments based on the defect location and classification was not significant (p-values of 0.87 and 0.26, respectively). Finally, the amount of deviation in our sample was significantly less than the reported average deviation (2 mm) from the reconstruction data in the literature by an average of −0.47 mm $p = 0.03$, 95 % (CI = -0.9–0.04).

3.3. Morphometric and 3D volumetric analysis

The mean difference between the intercondylar and intergonial distances of the pre- and post-operative models was 0.28 mm +/- 3.58 and −0.35 mm +/- 2.84 mm retrospectively. For the mandibular body length to the horizontal corner, the mean difference was 1.56 +/- 4.3 mm, and the mean difference to the midline was 0.2 +/- 2.84 mm. In addition, the average difference in the ramus length was 0.99 +/- 2.61 mm, and the mean sagittal angle discrepancy was −0.37 +/- 4.97 degrees. None of the linear and angular measurements showed a statistically significant deviation in the surgical result versus the virtual plan p-value > 0.05 (Table 2). The ICC showed excellent reliability in MRL (0.94) and MBL2 (0.96) measurements; good reliability in intercondylar distance (0.90); and moderate reliability in MBL1 (0.74), sagittal angle (0.87), and intergonial distance (0.82).

For volume deviation, the maximum negative deviation of the postoperative mandible ranged from −8.4 to −3.8 mm^3 with a mean of −6.0 +/- 1.5 mm^3 while the average maximum positive deviation was 5.6 +/- 2.27 mm^3 and a range of 1.8 to 9.6 mm^3. The mean of the deviation means of all models was −0.04 +/- 0.55 mm^3. There was no significant relationship between defect location or classification and volumetric deviation ($p > 0.05$). Finally, there were no significant correlations in the amount of deviation with any of the following variables: gender, diagnosis, reconstruction type, defect location, defect classification, and average 3D volume. The volume and morphometric measurements of the included subjects are shown in Table 3.

4. Discussion

Tumor margin status is critical in local tumor recurrence for both benign and malignant diseases and is a significant prognostic factor in head and neck cancer survival. Virtual surgical planning for ablative tumor resection was widely adopted before validating safety. This is especially a concerns in terms of the time to therapy initiation and the risk of tumor upstaging. (Farwell and Futran, 2000; Foley et al., 2013; Hanasono and Skoracki, 2013; Hassfeld and Mühling, 2001; Hassfeld et al., 1998) A recent study by Knitschke et al. showed that computer-assisted surgery and the observed time delay in the planning did not

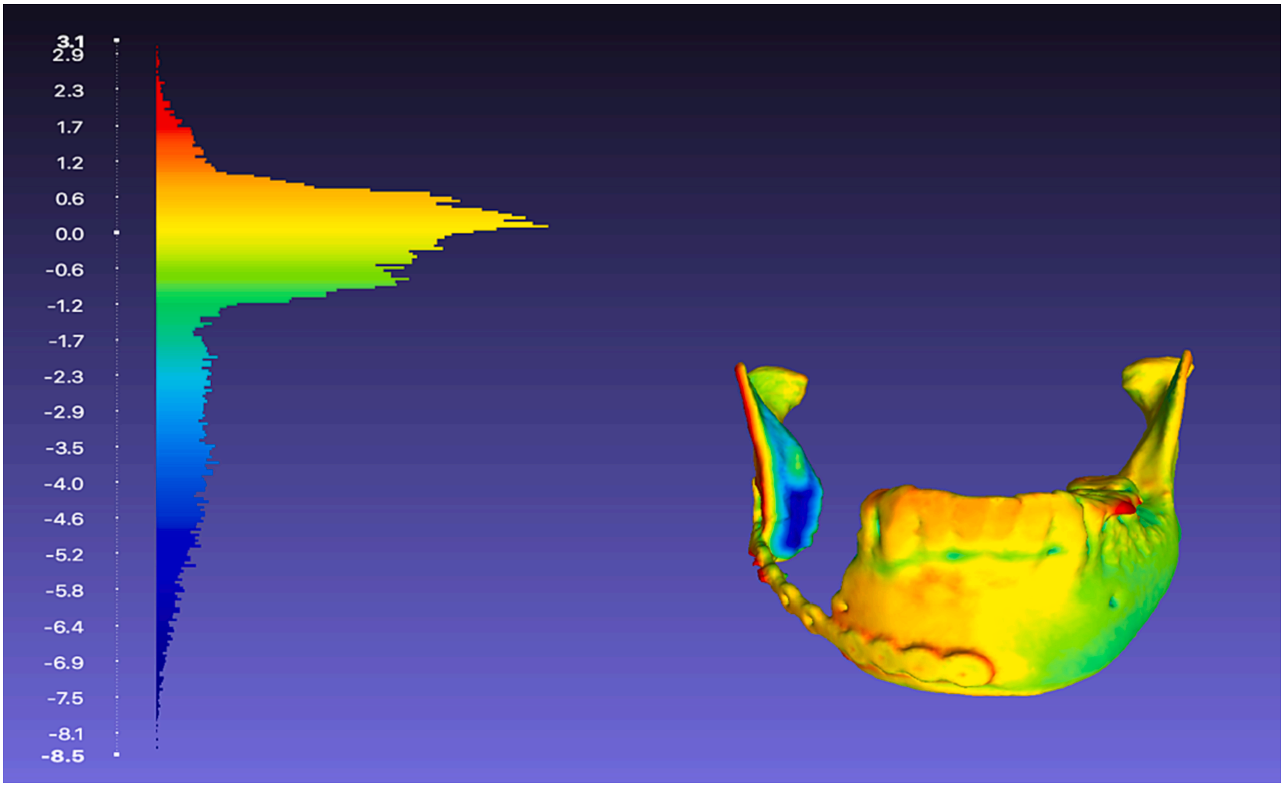

Fig. 3. Case example for the overall mandibular reconstruction accuracy. The histogram colormap shows 74.85 % of the deviation within 0.21 mm with a maximum positive deviation (red) at the lateral surface of the small segment and maximum negative deviation (blue) at the inner portion of the proximal segment cut. (For interpretation of the references to color in this figure legend, the reader is referred to the web version of this article.)

Table 2
Summary of the predictive demographic variables.

Variable	Value				
Age	48.5 +/- 23.8 (13-75)				
Gender	8 males (57.1%)		6 females (42.9%)		
Diagnosis	3 malignant (21.4%)	6 benign (42.9%)		5 osteonecrosis (35.7%)	
Location	5 laterals (35.7%)		9 combined central and lateral (64.3%)		
Reconstruction type	11 free flaps (78.5%)		3 non-free flaps (21.5%)		
Defect classification	3 class I (21.4%)	2 class Ic (14.3%)	2 class II (14.3%)	4 class III (28.6)	3 class IV (21.4%)
Number of segments	4 one segment (28.6%)	6 two segments (42.9%)		2 three segments (14.3%)	
Defect size	7.30 +/- 2.80 cm (4.4-12.2 cm)				

affect the margin status or the rate of lymph node metastasis in oral cancer patients. (Hinni et al., 2013) Similarly, the use of computer-assisted surgery did not lead to positive margin or recurrence in ameloblastoma resection (Huotilainen et al., 2014).

Despite the learning curve associated with computer-assisted surgery, the reported deviation from static virtual plan ranges from 0 to 12.5 mm and between 0.9° and 17.5° (Ciocca et al., 2016; Ibrahim et al., 2009; Knitschke et al., 2021; Koo and Li, 2016; Landaeta-Quinones et al., 2018; Liu et al., 2009; Marmulla et al., 1997; Marro et al., 2016; Maxwell et al., 2015; Mazzoni et al., 2013), while dynamic navigation has a more precise 2–5 mm replication of the plan. (Meier et al., 2005; Metzler et al., 2014; Modabber et al., 2014) These results indicate a wide range of deviation rate in the static version of computer-assisted surgery, which could potentially have a negative impact on patient outcomes.

Other confounding factors should also be considered that might contribute to the accurate placement of the cutting guides. As mentioned previously, the wide range of variations in the deviation measurement is due to utilizing different techniques. Looking at osteotomy deviation, Hanasono et al. reported a mean deviation of 2.4 +/- 2.06 mm for the actual versus projected fibular segment lengths and 3.51 +/- 2.69 degree in angle divergence. (Ibrahim et al., 2009) The repeatability of the isolated segments was 87.5 % within 1 mm and 96.5 % within 2 mm. (Palla and Callahan, 2021) Interestingly, other groups found that the fibular cut is more accurate (1.3–1.9 mm) than the mandibular osteotomy (2 – 2.3 mm). (Ciocca et al., 2016; Rodby et al., 2014) Our study has slightly more accurate results with 1.52 +/- 1.02 mm average deviation

Table 3
Full details of the volume and morphometric measurements of the included subjects.

	Volumetric analysis				Morphometric analysis					
Subject	Max -ve deviation	Max + ve deviation	Average deviation	% deviation	RL Δ	BL 1 Δ	BL 2 Δ	Sagittal angle Δ	IC Δ	IG Δ
1	−5.54	9.6	−0.14	35.45	3	N/A	N/A	N/A	−2	1
2	−6.45	4.8	0.06	57.88	1	0	−2	2.8	−4	−3
3	−5.27	7.95	0.17	41.21	3	10	−4	−1.4	−6	−4
4	−7.78	7	−1.3	44.8	1	4	3	−5.9	2	1
5	−4.6	1.8	0.11	73.1	0	1	−1	0.8	−5	1
6	−5.33	5.74	0.2	50	−2	1	3	−7.4	0	−1
7	−7.5	4.9	−0.95	61	4.1	−8	−1.4	−1.6	−1	−1
8	−4.37	3.3	−0.19	54.3	−1	2	0	0.7	0	−1
9	−5.83	6.86	0.51	50	0	−2	2.6	8.7	4	−6
10	−6.4	5.48	−0.49	50	4	3	3	5	1	1
11	−8.4	3.1	0.16	74.55	4.4	N/A	N/A	N/A	6	6
12	−3.81	6.32	0.73	44.84	−2	3	3	−3.3	2	−1
13	−8.4	3.1	0.21	74.85	2.4	−0.2	−3.2	3.8	3	1
14	−4.7	8.43	0.36	38.4	−4	5	4	−6.7	4	1

Abbreviations: Max: maximum, -ve: negative, +ve: positive, RL Δ: Ramus length difference, BL1 Δ: Body length 1 difference, BL2 Δ: Body length 2 difference, IC Δ: Intercondylar distance difference, IG Δ: Intergonial distance difference.

from the planned osteotomy cut most likely because the technology evolved, there was a better understanding of the cutting guide designs, and there was more precise and thinner metal guides with excellent adaptation.

Errors and imprecisions in computer-assisted surgery can develop at various phases perioperatively. Sometimes the error is cumulative or even detrimental to achieving an acceptable result. Initially, image acquisition, resolution, and processing flaws may lead to distortion in image data accuracy. (Roser et al., 2010) Pitch, gantry tilt, tube current, and voltage can also play a crucial role in image reconstructions. (Sawh-Martinez et al., 2017) In addition to the apparent effect of patient movement and metal artifacts, slice thickness is an integral component of the acquired image; ideally, the slice thickness should be less than 1.25 mm. (Chang et al., 2013; Choi et al., 2002).

Segmentation of the data set is highly influenced by the quality of the images and the segmentation tool used. DICOM files are converted to STL files via manual or automatic thresholding. (Schusterman et al., 1993; Shu et al., 2014) This can lead to enlargement, reduction, or distortion of the generated 3D object. For instance, different CT and CBCT machines and parameters can cause a geometrical deviation of more than 0.9 mm. (Stirling Craig et al., 2015) Typically, manual segmentation offers a better result with geometrical variations between STL models of 0.13 mm in medical grade computer tomography and 0.55 mm in CBCT. Nevertheless, manual segmentation is a subjective process, and Huotilainen et al. demonstrated inconsistency in geometry and size among three specialists who performed identical DICOM images conversion into a skull STL model. (Succo et al., 2015).

The printing process is another step and has dimensions (difference between the printed model's size and the STL model) approximately the size of an image voxel (1 mm). (Chang et al., 2013; Szewczyk et al., 2018) Lastly, the human error, accuracy method, and measurements instruments are important elements that can combine to measure the technology's accuracy during evaluation. (Taft et al., 2011) All previously mentioned steps in the preoperative planning, intraoperative execution, and postoperative analysis could potentially influence our results.

There is evident heterogeneity in the scientific literature in the method of comparing pre and postoperative data, which makes it challenging to compare studies. Typically, three common approaches are used: 1: comparing the pre and post DICOM images with each other (Knitschke et al., 2021; Tarsitano et al., 2018), 2: comparing the pre-STL model directly with the postoperative STL model with no regard to the virtual plan (original mandible not the neomandible) (Koo and Li, 2016; van Baar et al., 2018; van Baar et al., 2019; van Eijnatten et al., 2017), and 3: comparing the virtually-planned STL model to the postoperative STL model. (Ibrahim et al., 2009; van Eijnatten et al., 2017; Weitz et al., 2016; Whyms et al., 2013; Yu et al., 2016) If the goal is to examine the residual mandible, then the first two methods are valid; however, only the third technique allows for a proper assessment of the residual and neomandible, which is the ultimate purpose of evaluating the reconstruction goals such as facial harmony, function, and occlusion. (Zhang et al., 2016) Here, we elected to use the preoperative virtual plan with the postoperative 3D model because we wanted to assess how close we were in imitating the osteotomy line and evaluating the overall residual and neomandible volume.

Another aspect of the evaluation method is the superimposition of the STL models. Evaluating the reconstruction result based on volume superimposition eliminates the human error introduced by landmark selection. The superimposition can be fully automated using the iterative closest-point algorithm if there is considerable similarity between the two objects. In our study, we performed surface registration superimposition for the entire neomandible to evaluate the complete reconstruction. We also performed superimposition of the isolated parts of the remaining mandible after segmentation to look at each segment individually and measure the osteotomy deviation.

Despite our best efforts, several limitations still exist. Some are related to the study methodology, and others to the nature of the study design, lack of standardized evaluation tools, and limited resources. The study design is a retrospective single-center observation with no control group, which means that the results are not generalizable and prone to selection and observer bias. The imaging protocol was not standardized among the cases. Mixing CT scans with CBCT images produces distortion and altered spatial resolution. However, the inconsistency bias seems acceptable given that the slice thickness in all images is less than 1.25 mm. Finally, the measurements were validated with inter-observer assessment, but an accurate and reproducible evaluation tool does not exist. We tried to combine multiple evaluation techniques to overcome the deficiencies in some of the methods, but standardized subjective and objective guidelines are needed to enhance the research finding for comparison among future projects.

In conclusion, virtual surgical planning is an unambiguous paradigm shift in the predictability of the surgical plan and achievement of the reconstruction goals. The 3D printed cutting guides are a very accurate and reliable tool to help translate the bony surgical margin from a virtual plan to the actual surgical margin.

Data availability statement

The data that support the findings of this study are available from the corresponding author upon reasonable request.

Declaration of competing interest

The authors declare that they have no known competing financial interests or personal relationships that could have appeared to influence the work reported in this paper.

Acknowledgment

This study was approved by the Institutional Review Board of the University of Illinois at Chicago (UIC IRB Protocol #2019-0836). The authors received no financial support for the research or authorship of this study.

References

Abou-ElFetouh, A., Barakat, A., Abdel-Ghany, K., 2011. Computer-guided rapid-prototyped templates for segmental mandibular osteotomies: a preliminary report. Int J Med Robot. 7 (2), 187–192. https://doi.org/10.1002/rcs.387.

Ayoub, N., Ghassemi, A., Rana, M., et al., 2014. Evaluation of computer-assisted mandibular reconstruction with vascularized iliac crest bone graft compared to conventional surgery: a randomized prospective clinical trial. Trials. 15, 114. https://doi.org/10.1186/1745-6215-15-114.

Bak, M., Jacobson, A.S., Buchbinder, D., Urken, M.L., 2010. Contemporary reconstruction of the mandible. Oral Oncology. 46 (2), 71–76.

Bao, T., He, J., Yu, C., et al., 2017. Utilization of a pre-bent plate-positioning surgical guide system in precise mandibular reconstruction with a free fibula flap. Oral Oncology. 75, 133–139. https://doi.org/10.1016/j.oraloncology.2017.11.011.

Barker, T.M., Earwaker, W.J., Lisle, D.A., 1994. Accuracy of stereolithographic models of human anatomy. Australas Radiol. 38 (2), 106–111. https://doi.org/10.1111/j.1440-1673.1994.tb00146.x.

Barry, C.P., MacDhabheid, C., Tobin, K., et al., 2021. 'Out of house' virtual surgical planning for mandible reconstruction after cancer resection: is it oncologically safe? International Journal of Oral and Maxillofacial Surgery. 50 (8), 999–1002. https://doi.org/10.1016/j.ijom.2020.11.008.

Brown, J.S., Barry, C., Ho, M., Shaw, R., 2016. A new classification for mandibular defects after oncological resection. Lancet Oncol. 17 (1), e23–e30. https://doi.org/10.1016/S1470-2045(15)00310-1.

Chang, A.M.V., Kim, S.W., Duvvuri, U., et al., 2013. Early squamous cell carcinoma of the oral tongue: Comparing margins obtained from the glossectomy specimen to margins from the tumor bed. Oral Oncology. 49 (11), 1077–1082. https://doi.org/10.1016/j.oraloncology.2013.07.013.

Choi, J.Y., Choi, J.H., Kim, N.K., et al., 2002. Analysis of errors in medical rapid prototyping models. Int J Oral Maxillofac Surg. 31 (1), 23–32. https://doi.org/10.1054/ijom.2000.0135.

Ciocca, L., Marchetti, C., Mazzoni, S., et al., 2015. Accuracy of fibular sectioning and insertion into a rapid-prototyped bone plate, for mandibular reconstruction using CAD-CAM technology. Journal of Cranio-Maxillofacial Surgery. 43 (1), 28–33. https://doi.org/10.1016/j.jcms.2014.10.005.

Ciocca, L., Tarsitano, A., Marchetti, C., Scotti, R., 2016. A CAD–CAM-prototyped temporomandibular condyle connected to a bony plate to support a free fibula flap in patients undergoing mandiblectomy: A pilot study with 5 years of follow up. Journal of Cranio-Maxillofacial Surgery. 44 (7), 811–819. https://doi.org/10.1016/j.jcms.2016.04.030.

De Maesschalck, T., Courvoisier, D.S., Scolozzi, P., 2017. Computer-assisted versus traditional freehand technique in fibular free flap mandibular reconstruction: a morphological comparative study. European Archives of Oto-Rhino-Laryngology. 274 (1), 517–526. https://doi.org/10.1007/s00405-016-4246-4.

Disa, J.J., Winters, R.M., Hidalgo, D.A., 1997. Long-term evaluation of bone mass in free fibula flap mandible reconstruction. American Journal of Surgery. 174 (5), 503–506. https://doi.org/10.1016/S0002-9610(97)00152-9.

Eljamel, M.S., 1997. Accuracy, efficacy, and clinical applications of the Radionics Operating Arm System. Comput Aided Surg. 2 (5), 292–297. https://doi.org/10.1002/(SICI)1097-0150(1997)2:5<292::AID-IGS5>3.0.CO;2-V.

Farwell, D.G., Futran, N.D., 2000. Oromandibular Reconstruction. Facial Plast Surg. 16 (02), 115–126. https://doi.org/10.1055/s-2000-12573.

Foley, B.D., Thayer, W.P., Honeybrook, A., McKenna, S., Press, S., 2013. Mandibular reconstruction using computer-aided design and computer-aided manufacturing: an analysis of surgical results. J Oral Maxillofac Surg. 71 (2), e111–e119. https://doi.org/10.1016/j.joms.2012.08.022.

Hanasono, M.M., Skoracki, R.J., 2013. Computer-assisted design and rapid prototype modeling in microvascular mandible reconstruction. Laryngoscope. 123 (3), 597–604. https://doi.org/10.1002/lary.23717.

Hassfeld, S., Mühling, J., 2001. Computer assisted oral and maxillofacial surgery–a review and an assessment of technology. Int J Oral Maxillofac Surg. 30 (1), 2–13. https://doi.org/10.1054/ijom.2000.0024.

Hassfeld, S., Zöller, J., Albert, F.K., Wirtz, C.R., Knauth, M., Mühling, J., 1998. Preoperative planning and intraoperative navigation in skull base surgery. J Craniomaxillofac Surg. 26 (4), 220–225. https://doi.org/10.1016/s1010-5182(98)80017-6.

Hinni, M.L., Ferlito, A., Brandwein-Gensler, M.S., et al., 2013. Surgical margins in head and neck cancer: A contemporary review. Head & Neck. 35 (9), 1362–1370. https://doi.org/10.1002/hed.23110.

Huotilainen, E., Jaanimets, R., Valášek, J., et al., 2014. Inaccuracies in additive manufactured medical skull models caused by the DICOM to STL conversion process. J Craniomaxillofac Surg. 42 (5), e259–e265. https://doi.org/10.1016/j.jcms.2013.10.001.

Ibrahim, D., Broilo, T.L., Heitz, C., et al., 2009. Dimensional error of selective laser sintering, three-dimensional printing and PolyJet models in the reproduction of mandibular anatomy. J Craniomaxillofac Surg. 37 (3), 167–173. https://doi.org/10.1016/j.jcms.2008.10.008.

Knitschke, M., Bäcker, C., Schmermund, D., et al., 2021. Impact of Planning Method (Conventional versus Virtual) on Time to Therapy Initiation and Resection Margins: A Retrospective Analysis of 104 Immediate Jaw Reconstructions. Cancers. 13 (12), 3013. https://doi.org/10.3390/cancers13123013.

Koo, T.K., Li, M.Y., 2016. A Guideline of Selecting and Reporting Intraclass Correlation Coefficients for Reliability Research. J Chiropr Med. 15 (2), 155–163. https://doi.org/10.1016/j.jcm.2016.02.012.

Landaeta-Quinones, C.G., Hernandez, N., Zarroug, N.K., 2018. Computer-Assisted Surgery: Applications in Dentistry and Oral and Maxillofacial Surgery. Dental Clinics of North America. 62 (3), 403–420. https://doi.org/10.1016/j.cden.2018.03.009.

Liu, X. jing, Gui, L., Mao, C., Peng, X., Yu, G. yan, 2009. Applying computer techniques in maxillofacial reconstruction using a fibula flap: a messenger and an evaluation method. J Craniofac Surg. 20 (2), 372–377. https://doi.org/10.1097/SCS.0b013e31819b9443.

Marmulla, R., Hilbert, M., Niederdellmann, H., 1997. Inherent precision of mechanical, infrared and laser-guided navigation systems for computer-assisted surgery. J Craniomaxillofac Surg. 25 (4), 192–197. https://doi.org/10.1016/s1010-5182(97)80075-3.

Marro, A., Bandukwala, T., Mak, W., 2016. Three-Dimensional Printing and Medical Imaging: A Review of the Methods and Applications. Curr Probl Diagn Radiol. 45 (1), 2–9. https://doi.org/10.1067/j.cpradiol.2015.07.009.

Maxwell, J.H., Thompson, L.D.R., Brandwein-Gensler, M.S., et al., 2015. Early Oral Tongue Squamous Cell Carcinoma: Sampling of Margins From Tumor Bed and Worse Local Control. JAMA Otolaryngology-Head & Neck Surgery. 141 (12), 1104–1110. https://doi.org/10.1001/jamaoto.2015.1351.

Mazzoni, S., Marchetti, C., Sgarzani, R., Cipriani, R., Scotti, R., Ciocca, L., 2013. Prosthetically Guided Maxillofacial Surgery. Plastic and Reconstructive Surgery. 131 (6), 1376–1385. https://doi.org/10.1097/PRS.0b013e31828bd6b0.

Meier, J.D., Oliver, D.A., Varvares, M.A., 2005. Surgical margin determination in head and neck oncology: Current clinical practice. The results of an International American Head and Neck Society Member Survey. Head & Neck. 27 (11), 952–958. https://doi.org/10.1002/hed.20269.

Metzler, P., Geiger, E.J., Alcon, A., Ma, X., Steinbacher, D.M., 2014. Three-Dimensional Virtual Surgery Accuracy for Free Fibula Mandible Reconstruction: Planned Versus Actual Results. Journal of Oral and Maxillofacial Surgery. 72 (12), 2601–2612. https://doi.org/10.1016/j.joms.2014.07.024.

Modabber, A., Ayoub, N., Möhlhenrich, S.C., et al., 2014. The accuracy of computer-assisted primary mandibular reconstruction with vascularized bone flaps: iliac crest bone flap versus osteomyocutaneous fibula flap. Med Devices (auckl). 7, 211–217. https://doi.org/10.2147/MDER.S62698.

Palla, B., Callahan, N., 2021. Does the Use of Computer-Assisted Surgery Affect the Margin Status in Resections of Ameloblastoma? Journal of Oral and Maxillofacial Surgery. 79 (7), 1467–1473. https://doi.org/10.1016/j.joms.2020.09.007.

Rodby, K.A., Turin, S., Jacobs, R.J., et al., 2014. Advances in oncologic head and neck reconstruction: systematic review and future considerations of virtual surgical planning and computer aided design/computer aided modeling. Journal of Plastic, Reconstructive & Aesthetic Surgery. 67 (9), 1171–1185.

Roser, S.M., Ramachandra, S., Blair, H., et al., 2010. The accuracy of virtual surgical planning in free fibula mandibular reconstruction: comparison of planned and final results. Journal of Oral and Maxillofacial Surgery. 68 (11), 2824–2832.

Sawh-Martinez, R., Parsaei, Y., Wu, R., et al., 2017. Improved Temporomandibular Joint Position After 3-Dimensional Planned Mandibular Reconstruction. Journal of Oral and Maxillofacial Surgery. 75 (1), 197–206. https://doi.org/10.1016/j.joms.2016.07.032.

Schusterman, M.A., Harris, S.W., Raymond, A.K., Goepfert, H., 1993. Immediate free flap mandibular reconstruction: significance of adequate surgical margins. Head Neck. 15 (3), 204–207.

Shu, D. long, Liu, X. zhen, Guo, B., Ran, W., Liao, X., Zhang, Y. yan. 2014. Accuracy of using computer-aided rapid prototyping templates for mandible reconstruction with an iliac crest graft. World J Surg Oncol. 12, 190. doi:10.1186/1477-7819-12-190.

Stirling Craig, E., Yuhasz, M., Shah, A., et al., 2015. Simulated surgery and cutting guides enhance spatial positioning in free fibular mandibular reconstruction. Microsurgery. 35 (1), 29–33.

Succo, G., Berrone, M., Battiston, B., et al., 2015. Step-by-step surgical technique for mandibular reconstruction with fibular free flap: application of digital technology in virtual surgical planning. Eur Arch Otorhinolaryngol. 272 (6), 1491–1501. https://doi.org/10.1007/s00405-014-3078-3.

Szewczyk, M., Golusinski, W., Pazdrowski, J., Masternak, M., Sharma, N., Golusinski, P., 2018. Positive fresh frozen section margins as an adverse independent prognostic factor for local recurrence in oral cancer patients: Positive Fresh Frozen as an Adverse Factor. The Laryngoscope. 128 (5), 1093–1098. https://doi.org/10.1002/lary.26890.

Taft, R.M., Kondor, S., Grant, G.T., 2011. Accuracy of rapid prototype models for head and neck reconstruction. The Journal of Prosthetic Dentistry. 106 (6), 399–408. https://doi.org/10.1016/S0022-3913(11)60154-6.

Tarsitano, A., Battaglia, S., Ricotta, F., et al., 2018. Accuracy of CAD/CAM mandibular reconstruction: A three-dimensional, fully virtual outcome evaluation method.

Journal of Cranio-Maxillofacial Surgery. 46 (7), 1121–1125. https://doi.org/10.1016/j.jcms.2018.05.010.

van Baar, G.J.C., Forouzanfar, T., Liberton, N.P.T.J., Winters, H.A.H., Leusink, F.K.J., 2018. Accuracy of computer-assisted surgery in mandibular reconstruction: A systematic review. Oral Oncology. 84, 52–60. https://doi.org/10.1016/j.oraloncology.2018.07.004.

van Baar, G.J.C., Liberton, N.P.T.J., Forouzanfar, T., Winters, H.A.H., Leusink, F.K.J., 2019. Accuracy of computer-assisted surgery in mandibular reconstruction: A postoperative evaluation guideline. Oral Oncology. 88, 1–8. https://doi.org/10.1016/j.oraloncology.2018.11.013.

van Eijnatten, M., Berger, F.H., de Graaf, P., Koivisto, J., Forouzanfar, T., Wolff, J., 2017. Influence of CT parameters on STL model accuracy. Rapid Prototyping Journal. 23 (4), 678–685. https://doi.org/10.1108/RPJ-07-2015-0092.

van Eijnatten, M., Koivisto, J., Karhu, K., Forouzanfar, T., Wolff, J., 2017. The impact of manual threshold selection in medical additive manufacturing. Int J Comput Assist Radiol Surg. 12 (4), 607–615. https://doi.org/10.1007/s11548-016-1490-4.

Weitz, J., Bauer, F.J.M., Hapfelmeier, A., Rohleder, N.H., Wolff, K.D., Kesting, M.R., 2016. Accuracy of mandibular reconstruction by three-dimensional guided vascularised fibular free flap after segmental mandibulectomy. Br J Oral Maxillofac Surg. 54 (5), 506–510. https://doi.org/10.1016/j.bjoms.2016.01.029.

Whyms, B.J., Vorperian, H.K., Gentry, L.R., Schimek, E.M., Bersu, E.T., Chung, M.K., 2013. The effect of computed tomographic scanner parameters and 3-dimensional volume rendering techniques on the accuracy of linear, angular, and volumetric measurements of the mandible. Oral Surgery, Oral Medicine, Oral Pathology and Oral Radiology. 115 (5), 682–691. https://doi.org/10.1016/j.oooo.2013.02.008.

Yu, Y., Zhang, W.B., Liu, X.J., Guo, C.B., Yu, G.Y., Peng, X., 2016. Three-Dimensional Accuracy of Virtual Planning and Surgical Navigation for Mandibular Reconstruction With Free Fibula Flap. J Oral Maxillofac Surg. 74 (7), 1503.e1–1503.e10. https://doi.org/10.1016/j.joms.2016.02.020.

Zhang, W.B., Yu, Y., Wang, Y., et al., 2016. Improving the accuracy of mandibular reconstruction with vascularized iliac crest flap: Role of computer-assisted techniques. Journal of Cranio-Maxillofacial Surgery. 44 (11), 1819–1827. https://doi.org/10.1016/j.jcms.2016.08.014.